



Published in final edited form as:

Nat Med. 2008 December ; 14(12): 1351–1356. doi:10.1038/nm.1890.

Effective Use of PI3K and MEK Inhibitors to Treat Mutant K-Ras G12D and PIK3CA H1047R Murine Lung Cancers

Jeffrey A. Engelman^{1,2,3,*}, Liang Chen^{4,5,*}, Xiaohong Tan^{4,5}, Katherine Crosby⁶, Alexander R. Guimaraes⁷, Rabi Upadhyay⁷, Michel Maira⁸, Kate McNamara^{4,5}, Samantha A. Perera^{4,5}, Youngchul Song¹, Lucian R. Chiriac⁹, Ramneet Kaur¹, Angela Lightbown⁶, Jessica Simendinger⁶, Timothy Li², Robert F. Padera⁹, Carlos García-Echeverría⁸, Ralph Weissleder⁷, Umar Mahmood⁷, Lewis C. Cantley^{2,3,10,#}, and Kwok-Kin Wong^{3,4,5,#}

¹Massachusetts General Hospital Cancer Center, 149 13th Street, Charlestown, MA 02129, USA
²BIDMC Cancer Center, Beth Israel's Hospital, 77 Avenue Louis Pasteur Boston, MA 02115, USA
³Department of Medicine, Harvard Medical School, 25 Shattuck Street, Boston, MA 02115, USA
⁴Department of Medical Oncology, Dana-Farber Cancer Institute, 44 Binney Street, Boston, MA 02115, USA
⁵Ludwig Center at Dana-Farber/Harvard Cancer Center, 44 Binney Street, Boston, MA 02115, USA
⁶Cell Signaling Technology, 3 Trask Lane, Danvers, MA
⁷Center for Molecular Imaging Research, Massachusetts General Hospital, Harvard Medical School, 149 13th Street, Charlestown, MA 02129, USA
⁸Novartis Institutes for Biomedical Research, Oncology Disease Area, Klybeckstrasse 141, CH-4057 Basel, Switzerland
⁹Department of Pathology, Brigham and Women's Hospital, 75 Francis Street, Boston, MA 02115, USA
¹⁰Department of Systems Biology, Harvard Medical School, 200 Longwood Avenue, Boston, MA 02115, USA

Abstract

Somatic mutations that activate phosphoinositide 3-kinase (PI3K) have been identified in the p110- α catalytic subunit (*PIK3CA*) 1. They are most frequently observed in two hotspots: the helical domain (E545K and E542K) and the kinase domain (H1047R). Although the *PIK3CA* mutants are transforming *in vitro*, their oncogenic potential has not been assessed in genetically engineered mouse models. Furthermore, clinical trials with PI3K inhibitors have recently been initiated, and it is unknown if their efficacy will be restricted to specific, genetically defined malignancies. In this study, we engineered an inducible bitransgenic mouse model that develops lung adenocarcinomas initiated and maintained by expression of p110- α H1047R. Treatment of these tumors with NVP-BEZ235, a dual pan PI3K/mTOR inhibitor in clinical development, led to marked tumor regression as shown by PET-CT, MRI and microscopic examination. In contrast, mouse lung cancers driven by mutant *K-Ras* did not substantially respond to single-agent NVP-BEZ235. However, when NVP-BEZ235 was combined with a MEK inhibitor, ARRY-142886, there was dramatic synergy in shrinking these *K-Ras* mutant cancers. These *in vivo* studies suggest

Users may view, print, copy, and download text and data-mine the content in such documents, for the purposes of academic research, subject always to the full Conditions of use:http://www.nature.com/authors/editorial_policies/license.html#terms

Corresponding authors: Lewis C. Cantley, Beth Israel Deaconess Medical Center, New Research Building, Boston, MA 02115, Phone: (617) 667-0934, Fax: (617) 667-0957, E-mail: lewis_cantley@hms.harvard.edu, Kwok-Kin Wong, Dana-Farber Cancer Institute, Boston, MA 02115, Phone: (617)-632-6084, Fax, E-mail: KWONG1@PARTNERS.ORG.

*These authors contributed equally to this work

that inhibitors of the PI3K/mTOR pathway may be active in cancers with *PIK3CA* mutations, and, when combined with MEK inhibitors, may effectively treat *K-RAS* mutated lung cancers.

To generate mice with inducible expression of human p110 α H1047R, we injected a DNA segment consisting of seven direct repeats of the tetracycline (tet)-operator sequence, followed by *hPIK3CA H1047R* cDNA and *SV40 polyA* into FVB/N fertilized eggs as described previously 2,3 (Materials and Methods). Ten *Tet-op-hPIK3CA* founders were identified and then crossed to *CCSP-rtTA* mice (that specifically targets expression of the reverse tetracycline trans-activator protein (rtTA) in type II alveolar epithelial cells) to generate inducible, bitransgenic mouse cohorts harboring both the activator and the responder transgenes 4,5. The *Tet-op-hPIK3CA* copy numbers from the two most utilized founders were determined by quantitative real-time PCR (Supplementary Fig. 1a).

To induce expression p110- α H1047R in mouse lung epithelial cells, we administered doxycycline (doxy) to bitransgenic mice from each of the founder lines, monitored them for labored breathing, and imaged dyspneic mice with MRI to identify abnormalities. Three founder lines #13, #121, and #301 demonstrated labored breathing and MRI images consistent with lung tumors after 12, 26, and 60 weeks respectively. These mice were sacrificed, and gross inspection revealed multiple small tumor nodules. Histological analyses revealed mixed adenocarcinomas with bronchioloalveolar features (Fig. 1a). As founder line #13 demonstrated the shortest latency period, it was utilized for subsequent experiments.

The inducibility of the *PIK3CA* mutant transgene expression in the lung was evaluated at the RNA level using RT-PCR. *PIK3CA H1047R* expression was readily observed after 12 weeks of doxycycline administration (Supplementary Fig. 1b). Doxycycline withdrawal led to a loss of mutant *PIK3CA* expression. We observed expression of mutant p110- α protein in PI3K immunoprecipitations only from the bitransgenic mice induced with doxycycline (Supplementary Fig. 1c). Of note, expression of the transgene did not substantially increase total p110- α protein levels. This is expected since p110- α that is not bound to p85 is unstable, and any p110- α expressed in excess of p85 is rapidly degraded 6-8.

Withdrawal of doxycycline led to rapid and dramatic tumor regression thereby demonstrating that these established lung tumors require continued expression of p110- α H1047R (Fig. 1b). After doxycycline withdrawal, histological examination showed focal pulmonary fibrosis and scarring and no evidence of cancer (Fig. 1c). Of note, complete tumor regression was also observed in the other founder line (#121) that was examined for reversibility (Supplemental Fig. 2). Thus, these lung tumors require continued p110- α H1047R expression for their maintenance.

To inhibit PI3K signaling *in vivo*, we treated mice with NVP-BEZ235, a potent dual pan-PI3K/mTOR inhibitor currently under clinical development by Novartis Pharma Ag (Supplementary Fig. 3a) 9. This drug blocks the kinase activity of all four p110 isoforms and mutant p110- α H1047R with similar potencies 9. To identify a dose that adequately blocks PI3K in lung tissue, we treated control mice with one dose ranging from 30-52.5 mg/kg, and lungs were harvested either 3 or 8 hours later. At most of the dose levels examined, NVP-

BEZ235 induced suppression of PI3K signaling as indicated by decreased P-Akt levels (Supplementary Fig. 3b). We then evaluated if this compound could inhibit PI3K signaling in the lung tumors induced by the p110- α H1047R mutant. One oral treatment of NVP-BEZ235 35 mg/kg led to substantial suppression of Akt, S6, and 4e-bp1 phosphorylation in these mouse tumors (Fig. 2a).

We next evaluated the clinical efficacy of NVP-BEZ235 against p110- α H1047R induced mouse lung tumors. Tumor responses were assessed by MRI, PET-CT scans, and histological analyses. Doxycycline was administered to bitransgenic mice, and MRI screening identified mice with established tumors prior to initiating treatment. We observed that four days of treatment with NVP-BEZ235 at 35mg/kg per day led to a substantial reduction in the tumor's ^{18}F FDG avidity as measured by PET imaging and also led to a dramatic decrease in their size as judged by CT (Fig. 2b and Supplemental Movie for three dimensional reconstruction PET images). This data supports the notion that ^{18}F FDG-PET imaging may be an important pharmacodynamic marker for efficacy of PI3K inhibitors in the clinic. Histopathological analysis after short-term treatments demonstrate decreased cellularity and increased interstitial thickening within the residual tumor nodule with no evidence of adenocarcinoma (Fig. 2c).

Since NVP-BEZ235 is dual PI3K/mTOR inhibitor, we determined if the effects of this compound were due to its inhibition of TORC1 (mTOR/Raptor). Therefore, we treated mice with established *PIK3CA* mutated tumors with rapamycin. Treatment with rapamycin effectively blocked TORC1 in these tumors as evidenced by a loss of S6 phosphorylation (Supplementary Fig. 4). However, unlike NVP-BEZ235, rapamycin did not shrink these tumors (Figs. 2d,e). Thus, it appears that the activity of NVP-BEZ235 is not due solely to TORC1 inhibition.

Recently, a study by Downward and colleagues revealed that p110- α is required for lung tumorigenesis in the *LA2 K-Ras G12* mouse model 10. In that study, mice were generated in which the endogenous *Pik3ca* gene was mutated in the Ras binding domain. This mutation abrogated the ability of K-Ras G12D to induce lung tumors. Using a different genetic approach, we also observed that loss of PI3K signaling hindered K-Ras induced lung tumorigenesis. We crossed the LSL K-Ras mice to those with genetic deletion of the p85 PI3K regulatory subunits (encoded by *Pik3r1* and *Pik3r2*). We previously utilized p85 knockouts to genetically ablate PI3K signaling in different tumor models 11. The experiments were performed on a *Pik3r2* $^{-/-}$ background, and the *Pik3r1* allele was flanked by flox sites. Inhaled adenoviral Cre leads to both its deletion and activation of K-Ras G12D. We observed that loss of both *Pik3r1* alleles significantly inhibited tumorigenesis (Fig. 3a). Of note, these genetic experiments evaluate the role of PI3K in mutant K-Ras induced tumor *development*. To more closely mirror clinical treatment of patients with cancer, we evaluated if PI3K signaling was necessary for the maintenance of established K-Ras driven tumors. We utilized both the tet-inducible *K-Ras G12D* transgenic model 4 as well as the *LSL K-Ras* mouse model to induce lung tumors. After tumors developed, the mice were treated with the NVP-BEZ235. In contrast to the lung cancers induced by p110- α H1047R, those derived from K-Ras G12D did not shrink in response to single-agent BEZ235 as indicated by PET-CT or MRI images (Figs. 3b, c and S5a). However, NVP-

BEZ235 decreased Akt phosphorylation in these lungs as determined by western blot analysis (Fig. 3d) and immunohistochemical analysis (see below). These results suggest that PI3K may be required for K-Ras induced tumorigenesis, but may be less critical for tumor maintenance. Although both K-Ras tumor model mouse strains and the p110- α H1047R tumor model mouse strain are on similar mixed genetic backgrounds, it remains conceivable that subtle differences in genetic background may have affected responsiveness to PI3K inhibitors. However, the data with the K-Ras tumor models clearly underscores the notion that blocking tumorigenesis is not equivalent to treating a cancer that has already been established.

Recently, it has become evident that cancers respond dramatically to therapies targeting receptor tyrosine kinases (RTKs) when inhibition of the RTK leads to loss of both PI3K and ERK signaling 12-15. To recapitulate this effect in the K-Ras mutant lung tumors, we treated the mice with a combination of a PI3K and a MEK inhibitors. Whereas treatment of the K-Ras mutant mice with the MEK inhibitor, ARRY-142886 16, led to only modest tumor regression, the combination led to marked synergistic tumor regression (Figs. 4a,b), and pathological analyses at the completion of treatment revealed only scant remnants of tumor nodules (Supplementary Fig. 5b). After two days of the combination treatment, there was marked downregulation of PI3K, Erk and downstream signaling as indicated by western blot analyses and IHC (Figs. 4c,d). Of note, we invariably detected low level P-Akt staining in the K-Ras G12D nodules that was impressively lost upon treatment of the mouse with NVP-BEZ235 (Fig. 4d).

K-RAS mutated lung cancers remain a huge cancer problem as they comprise 20-30% of non-small cell lung cancers. Currently, there are no effective targeted therapies for this subset of cancers. In fact, the presence of *K-RAS* mutations only serves to identify those cancers that are likely *not* to respond to targeted therapies. The data in this study clearly demonstrate that the combination of PI3K and MEK inhibitors may be a very potent combination for these cancers. We hope this study spurs efforts to combine these classes of inhibitors for *K-RAS* mutated cancers.

There is not yet sufficient clinical data to determine if PI3K inhibitors will be powerful therapeutic agents as single-agent cancer therapies for patients or whether they will be effective only when combined with other targeted therapies. However, it is tempting to speculate that cancers that harbor activating mutations in *PIK3CA* or loss of PTEN may be particularly sensitive to PI3K inhibitors. Although this study suggest that cancers with *PIK3CA* mutations may respond to PI3K inhibitors, human cancers with *PIK3CA* mutations often harbor other known oncogenic mutations such as *K-RAS* (colon cancers) and *HER2* amplification (breast cancer) 17-19. These concordant oncogenic genetic changes may impact their responsiveness to PI3K inhibitors and possibly may necessitate combinations as was the case for effective treatment of the *K-Ras* mutated mouse lung cancers.

Materials and Methods

Plasmids for transgenic mice

Human *PI3KCA* was purchased from OpenBiosystems, H1047R point mutation was introduced using QuickChange kit from Stratagene following manufacturer's instruction. *PI3KCA* H1047R gene was cloned into the BamHI and HindIII site of pTRE-tight resulting in pTRE-tight-H1047R. XhoI release fragment from pTRE-tight-H1047R was gel purified for pronuclei injection at Transgenic core facility at Dana-Farber Cancer Institute.

Mouse cohorts

Tet-op PI3KCA H1047R (H1047R) mice were crossed to *CCSP-rtTA* mice (generously provided by Dr. Jeffery Whitsett at University of Cincinnati). Bi-transgenic mice (*Tet-op PI3KCA 1047R* and *CCSP-rtTA*) were administered doxycycline diet (Cat# c11300-2000i, Researchdiets) beginning at 22 days of age. MRI was used to determine tumor burden as described 2. *Tet-op K-ras* mice were generously provided by Dr. Harold Varmus. *LSL-K-Ras G12D* mice were kindly provided by Dr. Tyler Jacks. All of the mice used in these studies were mixed genetic backgrounds (mostly B6 and FVB) and treatment studies were performed on littermate controls. All mice were housed in the pathogen free environment at the Harvard School of Public Health. The mice were handled in strict accord with good animal practice as defined by the The Center for Animal Resources and Comparative Medicine (ARCM) at Harvard Medical School, and all animal work was done with ARCM approval.

Cancer therapy using inhibitors

The dual PI3K/mTOR inhibitor, NVP-BEZ235-AN (Novartis Institutes for Biomedical Research), was reconstituted in 1 volume of NMP (1-methyl-2-pyrrolidone : Fluka : #69118), and then add 9 volumes of PEG300 (Fluka: # 81160). Mice were administered the indicated dosage by oral gavage. The dosage indicates the amount of the free base. The MEK inhibitor ARRY-142886 (AZD6244) was purchased from commercial sources and reconstituted in 0.5% methyl cellulose (Fluka) + 0.4% polysorbate (Tween 80; Fluka) and administered at the indicated dosage by oral gavage. Rapamycin stock solution was prepared as 50mg/ml in 100% ethanol and was diluted to 1mg/ml immediately before used with 5% PEG400 (v/v), 5% Tween80 (v/v), mixed thoroughly then and administered by intraperitoneal injection at the indicated dosage. After treatment, mice were analyzed by MRI and PET-CT at different time points to determine the change in tumor burden. Sectioning was performed by the Department of Pathology at Brigham and Women's Hospital.

PET-CT scans

The mice were imaged using a Siemens Inveon PET-CT one hour post injection of approximately 500 μ Ci of 18 F¹⁸FDG (18 fluoro deoxyglucose). A PET scan was performed first. The PET was set to finish after 600-million events were recorded. List mode files were rebinned in 3D, and the subsequent sinograms were reconstructed using filtered back projection for quantification. Certain images were also reconstructed using 2DOSEM for

better visualization. Immediately after the PET scan, a CT scan was acquired. The x-ray source was set to a voltage and current of 70 kVp and 500 uA respectively, and it was positioned relative to the CCD detector camera and mouse such that the effective pixel size was 59.73 μm isotropically. The mouse's breathing rate was monitored using a BioVet (M2M Imaging), and the breathing signal was used to gate the CT. 360 projections were acquired with an exposure time of 320 ms. All projection data were reconstructed using filtered backprojection. The images were interpolated bilinearly, and filtered with a Shepp-Logan filter for higher resolution.

MRI and tumor volume measurement

MRI measurements were performed as described previously 2. Briefly, MRI measurements were performed using a 4.7 T Bruker Avance horizontal bore system equipped with a 200 mm inner diameter gradient set capable of 30G/cm gradient strength or a 7T Bruker Pharmascan system. The mice were anesthetized with 1% isoflurane in an oxygen/air mixture. The animals' respiratory and cardiac rates were monitored using Biotrig Software (4.7T) or SA Instruments monitoring device (Stony Brook, NY for 7T system). The animals were imaged on the 4.7T system with RARE sequence (TR = 2000 ms, TE effect = 25 ms) in the coronal and axial planes with a 1mm slice thickness and with the number of slices sufficient to cover the entire lungs, and with a matrix size of 128 \times 128, field of view (FOV) of 2.5 \times 2.5 cm². With the same geometry as described above, the animals were also imaged with a GEFI sequence (TR = 180 ms, TE = 2.2 ms) with respiratory and cardiac gating, in both the coronal and axial planes. For images acquired on the 7T system, RARE sequences after the intravenous administration of 0.3 mmol/kg Gd-DTPA (Magnevist) were performed in both coronal and axial planes with TR = 600 ms, TE = 15.3 ms, FOV 5.4 \times 4.0 cm, matrix size 256 \times 192, slice thickness 1.0 mm, 12 NEX, for a voxel size of 0.2 \times 0.2 \times 1.0 mm. Using the RARE sequence scans, volume measurements of the tumors were performed using in-house customized software and statistical analysis was performed using student exact t-tests.

Supplementary Material

Refer to Web version on PubMed Central for supplementary material.

Acknowledgments

This work was supported by NIH K08 grant CA120060-01 (JAE), American Association for Cancer Research (JAE), and the International Association for the Study of Lung Cancer (JAE), a prostate cancer P01 CA089021 (LCC), a pancreatic cancer P01 CA117969 (LCC) and R01 GM41890 (LCC), the DF/HCC Lung Cancer Specialized Program of Research Excellence (SPORE) grant P50 CA090578 (JAE and KKW), the DF/HCC Gastrointestinal Cancer SPORE grant P50 CA127003 (JAE, RW, UM and LCC), and U24-CA092782 (RW, UM, AG). KKW was supported by NIH grant K08 AG024004, R01 CA122794, R01 AG2400401, the Joan Scarangelo Foundation to Conquer Lung Cancer, the Cecily and Robert Harris Foundation, and the Flight Attendant Medical Research Institute.

References

1. Samuels Y, et al. High Frequency of Mutations of the PIK3CA Gene in Human Cancers. *Science*. 2004
2. Ji H, et al. The impact of human EGFR kinase domain mutations on lung tumorigenesis and in vivo sensitivity to EGFR-targeted therapies. *Cancer Cell*. 2006; 9:485–95. [PubMed: 16730237]

3. Li D, et al. Bronchial and peripheral murine lung carcinomas induced by T790M-L858R mutant EGFR respond to HKI-272 and rapamycin combination therapy. *Cancer Cell*. 2007; 12:81–93. [PubMed: 17613438]
4. Fisher GH, et al. Induction and apoptotic regression of lung adenocarcinomas by regulation of a K-Ras transgene in the presence and absence of tumor suppressor genes. *Genes Dev*. 2001; 15:3249–62. [PubMed: 11751631]
5. Perl AK, Tichelaar JW, Whitsett JA. Conditional gene expression in the respiratory epithelium of the mouse. *Transgenic Res*. 2002; 11:21–9. [PubMed: 11874100]
6. Yu J, et al. Regulation of the p85/p110 phosphatidylinositol 3'-kinase: stabilization and inhibition of the p110alpha catalytic subunit by the p85 regulatory subunit. *Mol Cell Biol*. 1998; 18:1379–87. [PubMed: 9488453]
7. Fruman DA, et al. Impaired B cell development and proliferation in absence of phosphoinositide 3-kinase p85alpha. *Science*. 1999; 283:393–7. [PubMed: 9888855]
8. Brachmann SM, Ueki K, Engelman JA, Kahn RC, Cantley LC. Phosphoinositide 3-kinase catalytic subunit deletion and regulatory subunit deletion have opposite effects on insulin sensitivity in mice. *Mol Cell Biol*. 2005; 25:1596–607. [PubMed: 15713620]
9. Maira SM, et al. Identification and characterization of NVP-BEZ235, a new orally available dual PI3K/mTor inhibitor with potent in vivo antitumor activity. *Mol Cancer Ther*. 2008 In Press.
10. Gupta S, et al. Binding of ras to phosphoinositide 3-kinase p110alpha is required for ras-driven tumorigenesis in mice. *Cell*. 2007; 129:957–68. [PubMed: 17540175]
11. Luo J, et al. Modulation of epithelial neoplasia and lymphoid hyperplasia in PTEN+/- mice by the p85 regulatory subunits of phosphoinositide 3-kinase. *Proc Natl Acad Sci U S A*. 2005; 102:10238–43. [PubMed: 16006513]
12. She Q, et al. The BAD protein integrates survival signaling by EGFR/MAPK and PI3K/Akt kinase pathways in PTEN-deficient tumor cells. *Cancer Cell*. 2005; 8:287–97. [PubMed: 16226704]
13. Mellingerhoff IK, et al. Molecular determinants of the response of glioblastomas to EGFR kinase inhibitors. *N Engl J Med*. 2005; 353:2012–24. [PubMed: 16282176]
14. Sharma SV, Fischbach MA, Haber DA, Settleman J. "Oncogenic shock": explaining oncogene addiction through differential signal attenuation. *Clin Cancer Res*. 2006; 12:4392s–4395s. [PubMed: 16857816]
15. Engelman JA. The role of phosphoinositide 3-kinase pathway inhibitors in the treatment of lung cancer. *Clin Cancer Res*. 2007; 13:s4637–40. [PubMed: 17671156]
16. Yeh TC, et al. Biological characterization of ARRY-142886 (AZD6244), a potent, highly selective mitogen-activated protein kinase kinase 1/2 inhibitor. *Clin Cancer Res*. 2007; 13:1576–83. [PubMed: 17332304]
17. Lievre A, et al. KRAS mutation status is predictive of response to cetuximab therapy in colorectal cancer. *Cancer Res*. 2006; 66:3992–5. [PubMed: 16618717]
18. Jhaver M, et al. PIK3CA mutation/PTEN expression status predicts response of colon cancer cells to the epidermal growth factor receptor inhibitor cetuximab. *Cancer Res*. 2008; 68:1953–61. [PubMed: 18339877]
19. Perez-Tenorio G, et al. PIK3CA mutations and PTEN loss correlate with similar prognostic factors and are not mutually exclusive in breast cancer. *Clin Cancer Res*. 2007; 13:3577–84. [PubMed: 17575221]

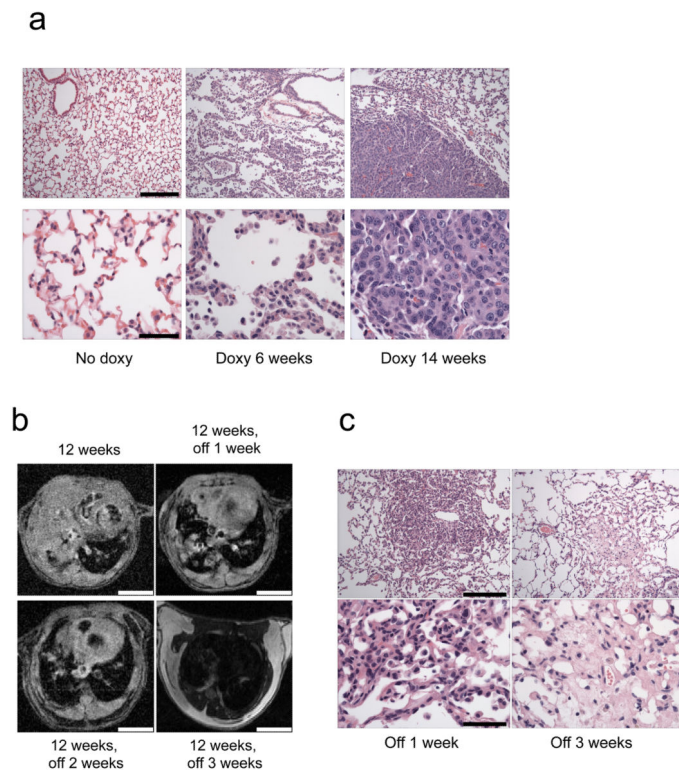


Figure 1. Development of a Tet-inducible *PIK3CA H1047R* mouse model of lung tumorigenesis (a) Histological analyses of lungs derived from the bitransgenic inducible *Tet-op-PIK3CA H1047R/CCSP-rtTA* (line #13) mice. Lungs from mice not induced with doxycycline, or those from mice induced for 6 and 14 weeks are shown. Adenocarcinoma is present in the lungs of mice induced with doxycycline after 6 and 14 weeks, respectively. Scale is 200 μM and 50 μM for upper and lower panels respectively. (b) Rapid disappearance of lung tumors following withdrawal of doxycycline. *PIK3CA H1047R/CCSP-rtTA* mice were placed on a doxycycline diet for 12 weeks to induce tumor formation, and tumors were assessed by MRI. The same mice were then taken off doxycycline and re-imaged 1, 2 and 3 weeks later. A representative example is shown. Scale is 4.5 mm. (c) Histological analysis of lungs after doxycycline withdrawal. *PIK3CA H1047R/CCSP-rtTA* mice were placed on a doxy diet until tumors were confirmed by MR imaging. Doxycycline was then withdrawn from their diets, the mice were sacrificed, and their lungs were examined histologically. Shown are the histology sections from two different mice after doxy withdrawal for 1 and 3 weeks respectively. Scale is 200 μM and 50 μM for upper and lower panels respectively.

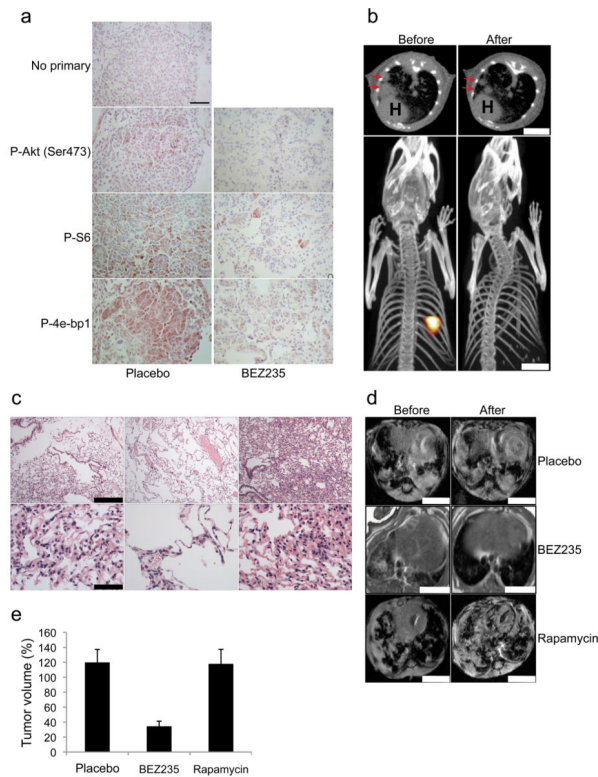


Figure 2. NVP-BEZ235 downregulates PI3K signaling in p110- α H1047R induced lung tumors and leads to rapid tumor regression

(a) *PIK3CA H1047R /CCSP-rtTA* tumors were induced in mice by feeding a doxy diet (verified by MR imaging). Mice with established tumors were treated with one dose of NVP-BEZ235 (35mg/kg) and the lungs were harvested 8 hours later. Sections were stained with the indicated antibodies. No primary was used as a control. Scale is 50 μ M. (b) *Tet-op PIK3CA H1047R /CCSP-rtTA* mice were treated with doxycycline until tumors developed. These tumors were imaged by both PET and CT scans (top and lower panels respectively). The mice were then treated with NVP-BEZ235 35mg/kg per day for four days and underwent repeat imaging. Red arrows on the CT scans indicate tumor, and **H**: Heart. Scale is 5 mm. (c) *PIK3CA H1047R /CCSP-rtTA* mice were treated with doxy until they developed tumors (confirmed by MRI). Mice with established tumors were treated with NVP-BEZ235 35mg/kg for 3 days (left and middle) or 2 days (right) and the lungs were examined histologically. Scale is 200 μ M and 50 μ M for upper and lower panels respectively. (d,e) *PIK3CA H1047R /CCSP-rtTA* mice with established tumors were treated with either placebo, NVP-BEZ235 35mg/kg or rapamycin 6 mg/kg daily for 2 weeks. (d) A representative MRI is shown before and after treatment for each group. Scales is 4.5 mm. (e) The average tumor volumes of three mice in each treatment group after 2 weeks are shown relative to pretreatment tumor volumes.

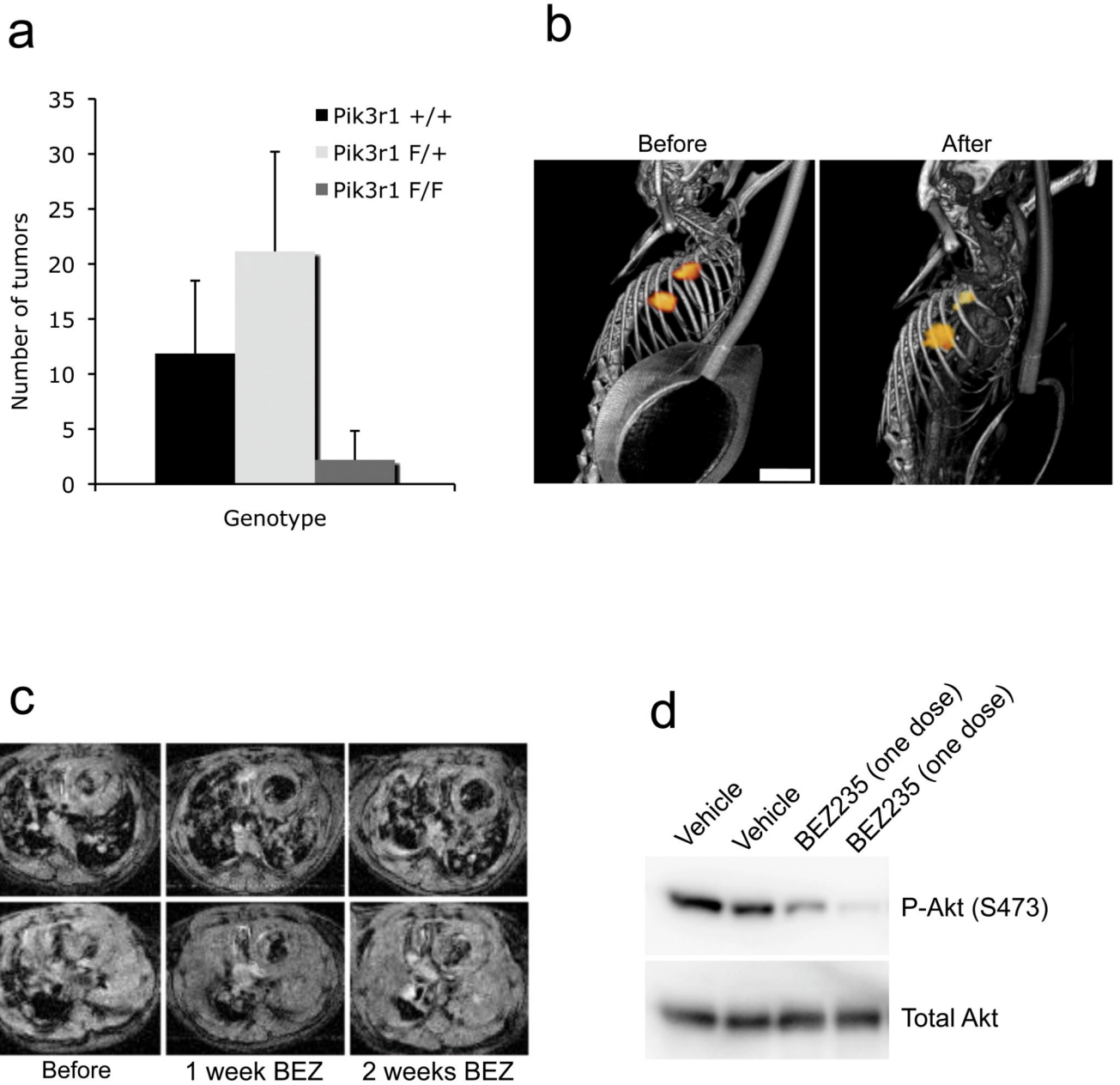


Figure 3. PI3K signaling is needed for K-Ras induced tumorigenesis but not tumor maintenance
(a) Genetic deletion of the PI3K regulatory subunit blocks K-Ras-induced tumorigenesis. *LSL K-Ras; Pik3r2*^{-/-} mice with either *Pik3r1*^{+/+} (n=7), *Pik3r1*^{F/+} (n=9), or *Pik3r1*^{F/F} (n=5) were treated with adenoviral Cre to induce lung tumors development. 15 weeks after adenoviral Cre inhalation, mice were sacrificed and tumor numbers were determined. The average number of tumors per mouse is shown for each genotype. **(b,c)** *Tet-op K-Ras* mice were induced to develop lung tumors with doxy, and then treated with NVP-BEZ235 35mg/kg for 2 weeks. **(b)** A PET-CT scan before and after one week of therapy is shown. Scale is 5 mm. **(c)** Axial MR images from two representative mice are displayed. Scale is 4.5 mm. **(d)** *Tet-op K-RasG12D/CCSP-rtTA* were induced to develop lung tumors on doxy

and then were treated with one dose of NVP-BEZ235 35mg/kg. Lungs were harvested 6 hours later and probed for P-Akt (Ser473) and Total Akt.

Author Manuscript

Author Manuscript

Author Manuscript

Author Manuscript

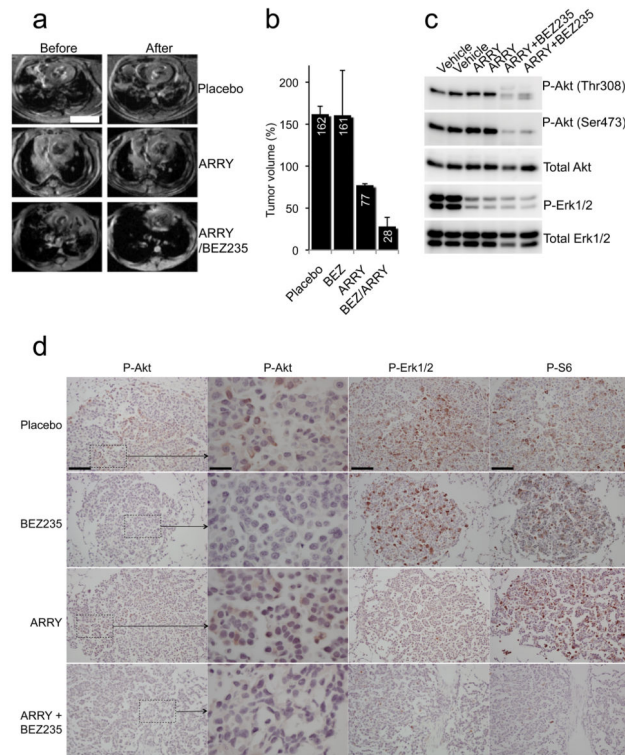


Figure 4. Combined PI3K and MEK inhibition dramatically shrinks K-Ras G12D induced lung tumors

(a,b) *LSL K-Ras* mice were induced to develop tumors by adenoviral Cre inhalation. After the establishment of sizeable tumors (determined by MRI), mice were treated with either placebo, NVP-BEZ235 35mg/kg once daily, ARRY-142886 25mg/kg twice daily, or NVP-BEZ235 35mg/kg once daily and ARRY-142886 25mg/kg once daily for two weeks. (a) Representative axial MRIs of the chest are shown. Scales is 4.5 mm. (b) The average tumor volumes of three mice in each treatment group after 2 weeks are shown relative to pretreatment tumor volumes. (c,d) Mice were treated as in (a) for 1.5 days. Six hours after their dose on day two of treatment, the animals were sacrificed. (c) One lung was snap-frozen in liquid nitrogen and assessed by western blotting using the indicated antibodies. (d) The other lung was fixed in formalin and assessed by immunohistochemistry (IHC) with the indicated antibodies. Microscopy was performed at two magnifications for the P-Akt IHC. The scale for the high magnification P-Akt IHC images is 25 μ m. The scale is 100 μ m for the other images. Hematoxylin and Eosin stains of the nodules examined by IHC are shown in the Supplemental Material (Supplementary Fig. 6).